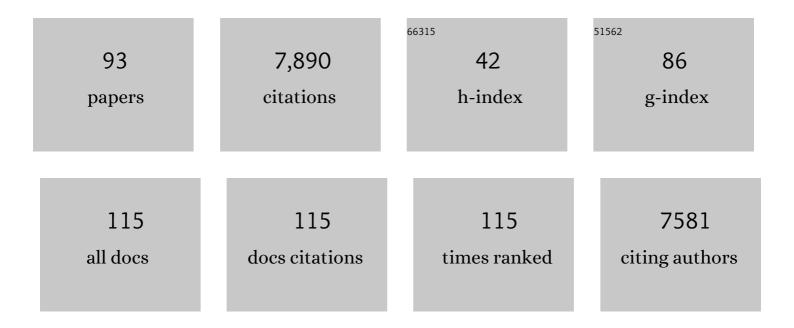
Isabel Trigo

List of Publications by Year in descending order

Source: https://exaly.com/author-pdf/1744576/publications.pdf Version: 2024-02-01



#	Article	IF	CITATIONS
1	Objective climatology of cyclones in the Mediterranean region: a consensus view among methods with different system identification and tracking criteria. Tellus, Series A: Dynamic Meteorology and Oceanography, 2022, 68, 29391.	0.8	79
2	Observed Landscape Responsiveness to Climate Forcing. Water Resources Research, 2022, 58, .	1.7	9
3	Integrating Reanalysis and Satellite Cloud Information to Estimate Surface Downward Long-Wave Radiation. Remote Sensing, 2022, 14, 1704.	1.8	8
4	A Comprehensive Clear-Sky Database for the Development of Land Surface Temperature Algorithms. Remote Sensing, 2022, 14, 2329.	1.8	1
5	A Practical Method for High-Resolution Burned Area Monitoring Using Sentinel-2 and VIIRS. Remote Sensing, 2021, 13, 1608.	1.8	14
6	Daily grass reference evapotranspiration with Meteosat Second Generation shortwave radiation and reference ET products. Agricultural Water Management, 2021, 248, 106543.	2.4	19
7	Validation and consistency assessment of land surface temperature from geostationary and polar orbit platforms: SEVIRI/MSG and AVHRR/Metop. ISPRS Journal of Photogrammetry and Remote Sensing, 2021, 175, 282-297.	4.9	15
8	Remote Sensing of Global Daily Evapotranspiration based on a Surface Energy Balance Method and Reanalysis Data. Journal of Geophysical Research D: Atmospheres, 2021, 126, e2020JD032873.	1.2	32
9	Upgrading Landâ€Cover and Vegetation Seasonality in the ECMWF Coupled System: Verification With FLUXNET Sites, METEOSAT Satellite Land Surface Temperatures, and ERA5 Atmospheric Reanalysis. Journal of Geophysical Research D: Atmospheres, 2021, 126, e2020JD034163.	1.2	17
10	Surface Albedo Retrieval from 40-Years of Earth Observations through the EUMETSAT/LSA SAF and EU/C3S Programmes: The Versatile Algorithm of PYALUS. Remote Sensing, 2021, 13, 372.	1.8	10
11	A deep learning approach for mapping and dating burned areas using temporal sequences of satellite images. ISPRS Journal of Photogrammetry and Remote Sensing, 2020, 160, 260-274.	4.9	63
12	A multi-sensor approach to retrieve emissivity angular dependence over desert regions. Remote Sensing of Environment, 2020, 237, 111559.	4.6	14
13	Multisensor Thermal Infrared and Microwave Land Surface Temperature Algorithm Intercomparison. Remote Sensing, 2020, 12, 4164.	1.8	4
14	Landâ€Atmosphere Drivers of Landscapeâ€Scale Plant Water Content Loss. Geophysical Research Letters, 2020, 47, e2020GL090331.	1.5	27
15	Google Earth Engine Open-Source Code for Land Surface Temperature Estimation from the Landsat Series. Remote Sensing, 2020, 12, 1471.	1.8	263
16	The roles of NDVI and Land Surface Temperature when using the Vegetation Health Index over dry regions. Global and Planetary Change, 2020, 190, 103198.	1.6	44
17	Enhancing the fire weather index with atmospheric instability information. Environmental Research Letters, 2020, 15, 0940b7.	2.2	16
18	Evaluation of Two Global Land Surface Albedo Datasets Distributed by the Copernicus Climate Change Service and the EUMETSAT LSA-SAF. Remote Sensing, 2020, 12, 1888.	1.8	9

#	Article	IF	CITATIONS
19	Role of vegetation in representing land surface temperature in the CHTESSEL (CY45R1) and SURFEX-ISBA (v8.1) land surface models: a case study over Iberia. Geoscientific Model Development, 2020, 13, 3975-3993.	1.3	25
20	A review of earth surface thermal radiation directionality observing and modeling: Historical development, current status and perspectives. Remote Sensing of Environment, 2019, 232, 111304.	4.6	91
21	Cold Bias of ERA5 Summertime Daily Maximum Land Surface Temperature over Iberian Peninsula. Remote Sensing, 2019, 11, 2570.	1.8	49
22	A New Retrieval Algorithm for Soil Moisture Index from Thermal Infrared Sensor On-Board Geostationary Satellites over Europe and Africa and Its Validation. Remote Sensing, 2019, 11, 1968.	1.8	12
23	A New Method to Estimate Reference Crop Evapotranspiration from Geostationary Satellite Imagery: Practical Considerations. Water (Switzerland), 2019, 11, 382.	1.2	15
24	Modelling of Wine Production Using Land Surface Temperature and FAPAR—The Case of the Douro Wine Region. Remote Sensing, 2019, 11, 604.	1.8	8
25	How well do global burned area products represent fire patterns in the Brazilian Savannas biome? An accuracy assessment of the MCD64 collections. International Journal of Applied Earth Observation and Geoinformation, 2019, 78, 318-331.	1.4	35
26	Satellite Retrieval of Downwelling Shortwave Surface Flux and Diffuse Fraction under All Sky Conditions in the Framework of the LSA SAF Program (Part 2: Evaluation). Remote Sensing, 2019, 11, 2630.	1.8	8
27	An All-Weather Land Surface Temperature Product Based on MSC/SEVIRI Observations. Remote Sensing, 2019, 11, 3044.	1.8	55
28	Satellite Retrieval of Downwelling Shortwave Surface Flux and Diffuse Fraction under All Sky Conditions in the Framework of the LSA SAF Program (Part 1: Methodology). Remote Sensing, 2019, 11, 2532.	1.8	8
29	Satelliteâ€Based Assessment of Land Surface Energy Partitioning–Soil Moisture Relationships and Effects of Confounding Variables. Water Resources Research, 2019, 55, 10657-10677.	1.7	37
30	Quantifying the Clearâ€Sky Bias of Satellite Land Surface Temperature Using Microwaveâ€Based Estimates. Journal of Geophysical Research D: Atmospheres, 2019, 124, 844-857.	1.2	29
31	Assessing the potential of parametric models to correct directional effects on local to global remotely sensed LST. Remote Sensing of Environment, 2018, 209, 410-422.	4.6	32
32	A Methodology to Simulate LST Directional Effects Based on Parametric Models and Landscape Properties. Remote Sensing, 2018, 10, 1114.	1.8	18
33	Fire danger rating over Mediterranean Europe based on fire radiative power derived from Meteosat. Natural Hazards and Earth System Sciences, 2018, 18, 515-529.	1.5	33
34	Satellite and In Situ Observations for Advancing Global Earth Surface Modelling: A Review. Remote Sensing, 2018, 10, 2038.	1.8	95
35	Land Surface Albedo Derived on a Ten Daily Basis from Meteosat Second Generation Observations: The NRT and Climate Data Record Collections from the EUMETSAT LSA SAF. Remote Sensing, 2018, 10, 1262.	1.8	21
36	Contribution of Land Surface Temperature (TCI) to Vegetation Health Index: A Comparative Study Using Clear Sky and All-Weather Climate Data Records. Remote Sensing, 2018, 10, 1324.	1.8	34

#	Article	IF	CITATIONS
37	A climatological assessment of drought impact on vegetation health index. Agricultural and Forest Meteorology, 2018, 259, 286-295.	1.9	118
38	Validation of reference evapotranspiration from Meteosat Second Generation (MSG) observations. Agricultural and Forest Meteorology, 2018, 259, 271-285.	1.9	31
39	Inversion of AMSRâ€E observations for land surface temperature estimation: 2. Global comparison with infrared satellite temperature. Journal of Geophysical Research D: Atmospheres, 2017, 122, 3348-3360.	1.2	22
40	Modelling directional effects on remotely sensed land surface temperature. Remote Sensing of Environment, 2017, 190, 56-69.	4.6	47
41	Advancing land surface model development with satellite-based Earth observations. Hydrology and Earth System Sciences, 2017, 21, 2483-2495.	1.9	39
42	Improving Land Surface Temperature Retrievals over Mountainous Regions. Remote Sensing, 2017, 9, 38.	1.8	9
43	A Physically Constrained Calibration Database for Land Surface Temperature Using Infrared Retrieval Algorithms. Remote Sensing, 2016, 8, 808.	1.8	13
44	Long Term Validation of Land Surface Temperature Retrieved from MSG/SEVIRI with Continuous in-Situ Measurements in Africa. Remote Sensing, 2016, 8, 410.	1.8	100
45	Downscaling Meteosat Land Surface Temperature over a Heterogeneous Landscape Using a Data Assimilation Approach. Remote Sensing, 2016, 8, 586.	1.8	7
46	The summer diurnal cycle of coastal cloudiness over west Iberia using Meteosat/SEVIRI and a WRF regional climate model simulation. International Journal of Climatology, 2016, 36, 1755-1772.	1.5	13
47	A Thermodynamically Based Model for Actual Evapotranspiration of an Extensive Grass Field Close to FAO Reference, Suitable for Remote Sensing Application. Journal of Hydrometeorology, 2016, 17, 1373-1382.	0.7	33
48	Comparison of model land skin temperature with remotely sensed estimates and assessment of surfaceâ€atmosphere coupling. Journal of Geophysical Research D: Atmospheres, 2015, 120, 12,096.	1.2	73
49	Quality assessment and improvement of the EUMETSAT Meteosat Surface Albedo Climate Data Record. Atmospheric Measurement Techniques, 2015, 8, 4561-4571.	1.2	10
50	Quality Assessment of S-NPP VIIRS Land Surface Temperature Product. Remote Sensing, 2015, 7, 12215-12241.	1.8	54
51	Meteosat Land Surface Temperature Climate Data Record: Achievable Accuracy and Potential Uncertainties. Remote Sensing, 2015, 7, 13139-13156.	1.8	74
52	Kalman filter physical retrieval of surface emissivity and temperature from SEVIRI infrared channels: a validation and intercomparison study. Atmospheric Measurement Techniques, 2015, 8, 2981-2997.	1.2	47
53	Validation of remotely sensed surface temperature over an oak woodland landscape — The problem of viewing and illumination geometries. Remote Sensing of Environment, 2014, 148, 16-27.	4.6	105
54	Calibration of the Fire Weather Index over Mediterranean Europe based on fire activity retrieved from MSG satellite imagery. International Journal of Wildland Fire, 2014, 23, 945.	1.0	35

#	Article	IF	CITATIONS
55	Satellite-derived land surface temperature: Current status and perspectives. Remote Sensing of Environment, 2013, 131, 14-37.	4.6	1,545
56	IMILAST: A Community Effort to Intercompare Extratropical Cyclone Detection and Tracking Algorithms. Bulletin of the American Meteorological Society, 2013, 94, 529-547.	1.7	391
57	Land surface temperature from multiple geostationary satellites. International Journal of Remote Sensing, 2013, 34, 3051-3068.	1.3	85
58	Are Greenhouse Gas Signals of Northern Hemisphere winter extra-tropical cyclone activity dependent on the identification and tracking algorithm?. Meteorologische Zeitschrift, 2013, 22, 61-68.	0.5	77
59	Kalman filter physical retrieval of surface emissivity and temperature from geostationary infrared radiances. Atmospheric Measurement Techniques, 2013, 6, 3613-3634.	1.2	61
60	Explosive development of winter storm Xynthia over the subtropical North Atlantic Ocean. Natural Hazards and Earth System Sciences, 2013, 13, 2239-2251.	1.5	56
61	Incoming Solar and Infrared Radiation Derived from METEOSAT: Impact on the Modeled Land Water and Energy Budget over France. Journal of Hydrometeorology, 2012, 13, 504-520.	0.7	37
62	Large-Scale Atmospheric Circulation Driving Extreme Climate Events in the Mediterranean and its Related Impacts. , 2012, , 347-417.		25
63	An innovative physical scheme to retrieve simultaneously surface temperature and emissivities using high spectral infrared observations from IASI. Journal of Geophysical Research, 2012, 117, .	3.3	22
64	Klaus – an exceptional winter storm over northern Iberia and southern France. Weather, 2011, 66, 330-334.	0.6	83
65	The Satellite Application Facility for Land Surface Analysis. International Journal of Remote Sensing, 2011, 32, 2725-2744.	1.3	207
66	Land surface albedo and downwelling shortwave radiation from MSG geostationary satellite: Method for retrieval, validation, and application. , 2011, , .		0
67	The state of climate in NW Iberia. Climate Research, 2011, 48, 109-144.	0.4	77
68	Reference crop evapotranspiration derived from geo-stationary satellite imagery: a case study for the Fogera flood plain, NW-Ethiopia and the Jordan Valley, Jordan. Hydrology and Earth System Sciences, 2010, 14, 2219-2228.	1.9	44
69	Estimation of downward longâ€wave radiation at the surface combining remotely sensed data and NWP data. Journal of Geophysical Research, 2010, 115, .	3.3	26
70	Synergistic use of the two-temperature and split-window methods for land-surface temperature retrieval. International Journal of Remote Sensing, 2010, 31, 4387-4409.	1.3	10
71	Quantifying the Uncertainty of Land Surface Temperature Retrievals From SEVIRI/Meteosat. IEEE Transactions on Geoscience and Remote Sensing, 2010, 48, 523-534.	2.7	142
72	Rainfall patterns and critical values associated with landslides in Povoação County (São Miguel) Tj ETQq0 0 0	rgBT /Ov 1.1	erlock 10 Tf 5 73

478-494.

#	Article	IF	CITATIONS
73	The Impact of North Atlantic Wind and Cyclone Trends on European Precipitation and Significant Wave Height in the Atlantic. Annals of the New York Academy of Sciences, 2008, 1146, 212-234.	1.8	99
74	Thermal Land Surface Emissivity Retrieved From SEVIRI/Meteosat. IEEE Transactions on Geoscience and Remote Sensing, 2008, 46, 307-315.	2.7	99
75	Correction of 2Âm-temperature forecasts using Kalman Filtering technique. Atmospheric Research, 2008, 87, 183-197.	1.8	33
76	An assessment of remotely sensed land surface temperature. Journal of Geophysical Research, 2008, 113, .	3.3	210
77	The Outstanding 2004/05 Drought in the Iberian Peninsula: Associated Atmospheric Circulation. Journal of Hydrometeorology, 2007, 8, 483-498.	0.7	208
78	On precursors of South American cyclogenesis. Tellus, Series A: Dynamic Meteorology and Oceanography, 2007, 59, 114-121.	0.8	30
79	Understanding Precipitation Changes in Iberia in Early Spring: Weather Typing and Storm-Tracking Approaches. Journal of Hydrometeorology, 2006, 7, 101-113.	0.7	184
80	Climatology and interannual variability of storm-tracks in the Euro-Atlantic sector: a comparison between ERA-40 and NCEP/NCAR reanalyses. Climate Dynamics, 2006, 26, 127-143.	1.7	244
81	Chapter 3 Relations between variability in the Mediterranean region and mid-latitude variability. Developments in Earth and Environmental Sciences, 2006, , 179-226.	0.1	71
82	Chapter 6 Cyclones in the Mediterranean region: Climatology and effects on the environment. Developments in Earth and Environmental Sciences, 2006, 4, 325-372.	0.1	99
83	The Influence of the North Atlantic Oscillation on Rainfall Triggering of Landslides near Lisbon. Natural Hazards, 2005, 36, 331-354.	1.6	73
84	Shallow and deep landslides induced by rainfall in the Lisbon region (Portugal): assessment of relationships with the North Atlantic Oscillation. Natural Hazards and Earth System Sciences, 2005, 5, 331-344.	1.5	190
85	Intercalibration of NOAA and Meteosat window channel brightness temperatures. International Journal of Remote Sensing, 2005, 26, 3717-3733.	1.3	13
86	How exceptional was the early August 2003 heatwave in France?. Geophysical Research Letters, 2005, 32, .	1.5	203
87	Climate impact of the European winter blocking episodes from the NCEP/NCAR Reanalyses. Climate Dynamics, 2004, 23, 17-28.	1.7	187
88	Clear-Sky Window Channel Radiances: A Comparison between Observations and the ECMWF Model. Journal of Applied Meteorology and Climatology, 2003, 42, 1463-1479.	1.7	29
89	Climatology of Cyclogenesis Mechanisms in the Mediterranean. Monthly Weather Review, 2002, 130, 549-569.	0.5	275
90	Meteorological conditions associated with sea surges in Venice: a 40 year climatology. International Journal of Climatology, 2002, 22, 787-803.	1.5	47

#	Article	IF	CITATIONS
91	Decline in Mediterranean rainfall caused by weakening of Mediterranean cyclones. Geophysical Research Letters, 2000, 27, 2913-2916.	1.5	124
92	Objective Climatology of Cyclones in the Mediterranean Region. Journal of Climate, 1999, 12, 1685-1696.	1.2	383
93	Moisture Sources and Large-Scale Dynamics Associated With a Flash Flood Event. Geophysical Monograph Series, 0, , 111-126.	0.1	30